

# NUMERICAL MODELLING OF BLAST RESISTANCE OF FRC AND REINFORCED CONCRETE SPECIMENS

M. Foglar<sup>1</sup>, M. Kovář<sup>2</sup>

## Abstract

*According to recent publications, from 2005 to 2008 there were more than 13000 terrorist attacks around the world, which took more than 73000 human lives. The attacks were targeted mainly on the technical and civic infrastructure, like governmental buildings, bridges, etc.*

*Due to improved ductility, fibre-reinforced concrete (FRC) shows better performance under blast and impact loading than conventionally reinforced concrete. Field tests of FRC and reinforced concrete specimens were performed in cooperation with the Czech Army corps and Police of the Czech Republic in the military training area Boletice. The test were performed using real scale precast slabs and 25 kg of TNT charges placed in distance from the slab for better simulation of real in-situ conditions.*

*The paper presents results of the tests and describes the methods of modeling the behaviour of reinforced concrete specimens and fiber reinforced concrete specimens under blast loading.*

**Keywords:** blast loading, fibre concrete, reinforced concrete, numerical modelling

## 1. Introduction

Recent terrorist attacks on railway and subway stations in Moscow (2011), Stockholm (2010), London (2005), Madrid (2004), etc. show great vulnerability of civil and transport infrastructure to this kind of threat. Attacks on structures like airports, railway and subway stations, bridges and governmental building can cause great casualties. These causalities are multiplied when the explosion causes collapse of the entire structure.

In case of new structures, the ductility needed for sustaining the extreme load caused by blast pressure wave can be achieved by using plastic fibers in the concrete mix. Even bigger increase of blast and impact performance can be achieved by the use of ultra high performance fiber-reinforced concrete or engineered cementitious composites (Millard & al., 2010).

---

<sup>1</sup> Ing. Marek Foglar, Ph.D., Czech Technical University in Prague, Faculty of Civil Engineering, Department of Concrete and Masonry Structures, Thakurova 7, 166 29 Praha 6, [marek.foglar@fsv.cvut.cz](mailto:marek.foglar@fsv.cvut.cz)

<sup>2</sup> Ing. Martin Kovář, Czech Technical University in Prague, Faculty of Civil Engineering, Department of Concrete and Masonry Structures, Thakurova 7, 166 29 Praha 6, [martin.kovar@fsv.cvut.cz](mailto:martin.kovar@fsv.cvut.cz)

This paper presents results of field tests of blast performance of reinforced concrete and reinforced concrete specimens with plastic fibers. The tests were performed in cooperation with the Czech Army corps and Police of the Czech Republic at the military training area Boletice using real scale precast slabs and 25 kg of TNT charges placed in distance from the slab for better simulation of real in-situ conditions.

## **2. Field tests of blast performance of reinforced concrete and reinforced concrete specimens with plastic fibres**

This section presents a brief summary of field tests of blast performance of reinforced concrete and reinforced concrete specimens with plastic fibers. The tests were performed in cooperation with the Czech Army corps and Police of the Czech Republic at the military training area Boletice using real scale precast slabs and 25 kg of TNT charges placed in distance from the slab for better simulation of real in-situ conditions. For detailed description, see Foglar et al. (2011).

### **2.1 Specimens**

Dimensions of the specimens were designed in real scale of a small span bridge in as concrete slabs, 6m long, 1,5m wide and 0,3m thick.

The specimens were made of C30/37-X0 concrete. Both specimens were reinforced by conventional reinforcement at both surfaces. The shear reinforcement was provided by  $\varnothing 8$ mm links (9pcs/m<sup>2</sup>).

Polypropylene 54mm long synthetic fibers at 4,5kg/m<sup>3</sup> (manufacturer Forta Ferro) were used in the second specimen.

### **2.2 Layout of the experiments**

The slabs were placed on timber posts which were fixed in position by steel tubes. The ground under the slabs was removed; 5m in diameter and 1m deep excavation was prepared under the slabs so the results of the experiments would not be influenced by rebound of the pressure wave.

The 25kg TNT charges were placed on steel “chairs” in the middle of the slabs. The “chairs” provided off stand of 450mm from the slab.

Layout of the experiments can be seen in Fig. 1.



*Fig. 1:* Layout of the experiments.

The charges were fired remotely by radio impulse.

### 2.3 Results of the experiments

The experiments showed the beneficiary effect of added fibers on blast performance of the specimens. The differences in puncture and spalling of concrete on the soffit of the slabs can be found in Tab. 1. The different effect of the blast on the surface closer to the explosion can be seen in Fig. 2 and 3.

Tab. 1: Comparison of blast performance of RC and RC with plastic fibers.

Damage	RC specimen	RC with plastic fibers	RC with fibers / RC
Puncture – top surface	0,43 m <sup>2</sup>	0,26 m <sup>2</sup>	60%
Permanent deflection	0,31 m	0,378 m	122%
Concrete spalling (soffit) - < concrete cover	2,35 m <sup>2</sup>	1,89 m <sup>2</sup>	80%
Concrete spalling (soffit) - > concrete cover	1,71 m <sup>2</sup>	1,09 m <sup>2</sup>	64%
Concrete spalling (left side) - < concrete cover	0,35 m <sup>2</sup>	0	-
Concrete spalling (left side) - > concrete cover	0,52 m <sup>2</sup>	0,05 m <sup>2</sup>	10%
Concrete spalling (right side) - < concrete cover	0,23 m <sup>2</sup>	0,11 m <sup>2</sup>	48%
Concrete spalling (right side) - > concrete cover	0,34 m <sup>2</sup>	0,16 m <sup>2</sup>	47%

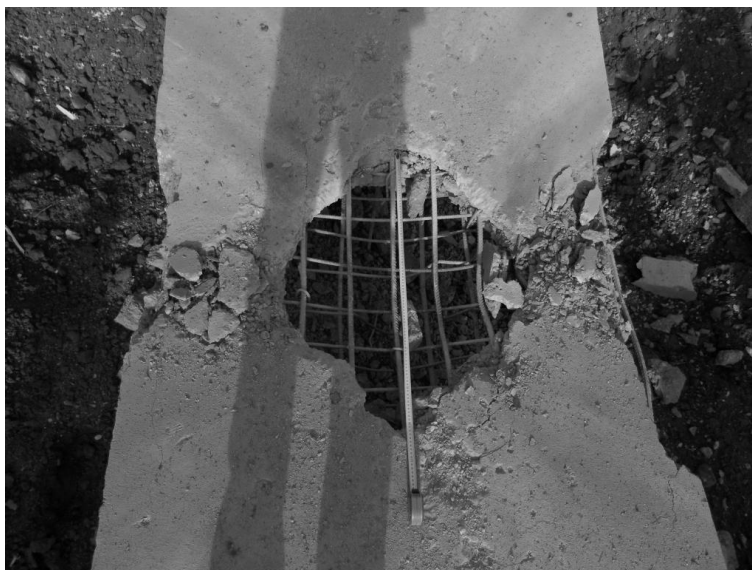


*Fig. 2:* Top surface of the RC specimen after the blast.

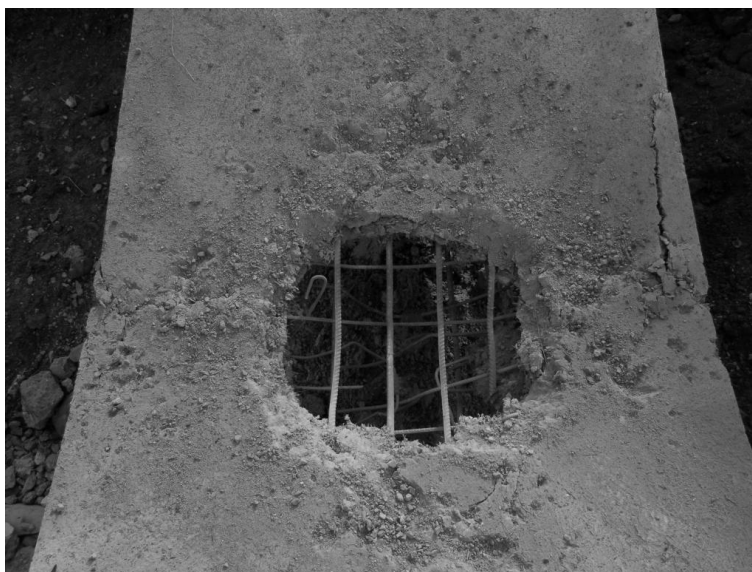


*Fig. 3:* Top surface of the RC specimen with plastic fibers after the blast.

### 3. Numerical modeling

A numerical model of the experiment was prepared for the purpose of further research. The process of model set-up is described in the following text. The model was calibrated according to the outcomes of the experiments described in the previous chapter.

#### 3.1 Numerical solution of fast dynamic phenomena

Fast dynamic phenomena can be solved by the method of explicit time integration (finite difference method, differential method, see Fig, 4) the equation of motion can be expressed as

$$M_n \cdot u_n'' + C_n \cdot u_n' + K_n \cdot u_n = p_n \quad (1)$$

is solved in time  $t_n$ , hence at the start of fixed time step.

The method is based on linear displacement change. The velocity

$$u'_{n+1/2} = \frac{1}{\Delta t_{n+1/2}} (u_{n+1} - u_n) \quad (2)$$

is inserted into equation of acceleration

$$u'' = \frac{1}{\Delta t_n} (u'_{n+1/2} - u'_{n-1/2}) \quad (3)$$

$u_{n+1}$  remains unknown in Eq. (1). The displacement in time  $t_{n+1}$  is

$$\left( \frac{1}{\Delta t^2} M_n + \frac{1}{2\Delta t} C_n \right) \cdot u_{n+1} = \quad (4)$$

$$P_n - \left( K_n - \frac{2}{\Delta t^2} M_n \right) \cdot u_n - \left( \frac{1}{\Delta t^2} M_n - \frac{1}{2\Delta t} C_n \right) \cdot u_{n-1}$$

The matrixes M and C are diagonal; the solution is fast and simple.

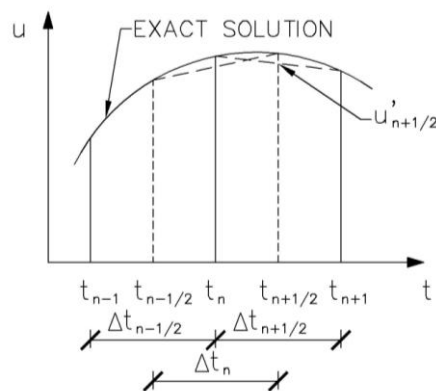


Fig. 4: The explicit time integration method (finite difference method)

In the method of explicit time integration, the system is in equilibrium only at time  $t_n$ , but not at time  $t_{n+1}$ . The time step depends on the highest natural frequency of the structural system. If the time step is adequately small, the method is numerically stable. The method of explicit time integration solves small number of equations in very small time steps in duration of approximately  $10^{-6} - 10^{-8}$  s. The method of explicit time integration is suitable only for processes of a very short duration.

### 3.2 Numerical modeling

LS-DYNA solver was developed for non-linear analysis of fast dynamic phenomena like blast or impact. Within the calculation, the FEM mesh can adapt by deleting elements whose resistance was depleted; this FEM elements “erode”.

The model consists of several parts. The air forms provides boundaries of the model; the explosive (e.g. TNT) transfers the energy from the blast to FE elements of the air, where the blast wave propagates. The concrete specimen is modeled by solids, for example of the model, see Fig. 5.

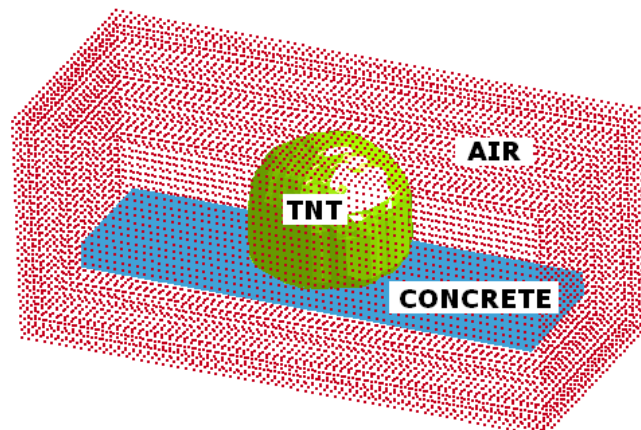


Fig. 5: Set-up of the FE model

The air is modeled using the 009-Null material and forms the undeformable FE network,. The concrete specimen is modeled by the 159- CSCM\_Concrete material model. The explosive is modeled by the 008-High explosive burn material model. The blast overpressure is calculated by the JWL equation of state (EOS):

$$p = A \left( 1 - \frac{\omega}{R_1 V} \right) e^{-R_1 V} + B \left( 1 - \frac{\omega}{R_2 V} \right) e^{-R_2 V} + \frac{\omega E}{V} \quad (5)$$

### 3.2.1 2D model

As the first step, a 2D model was prepared. Its goal was to show basic characteristics of the experiment, e.g. the time when the blast overpressure wave reaches the surface of the specimen, the time when the elements at the soffit the specimen start to erode, etc.

The blast overpressure wave reaches the surface of the specimen at 0,25 ms, see Fig. 6.

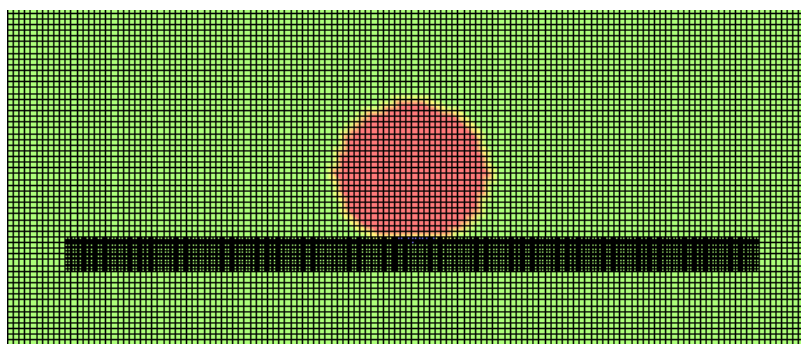
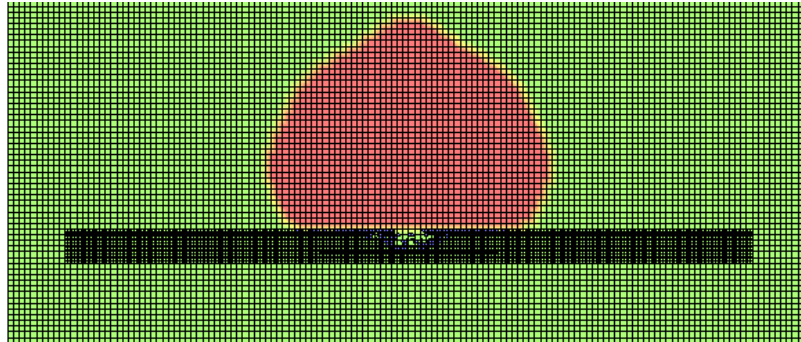


Fig. 6: Blast overpressure wave at 0,25 ms

The first finite elements start to erode at 0,4 ms, see Fig. 7.



*Fig. 7: Blast overpressure wave at 0,5 ms*

Fig. 8 compares the recorded blast overpressure wave during the experiment with the FE model; element erosion can be spotted under the hypocenter.

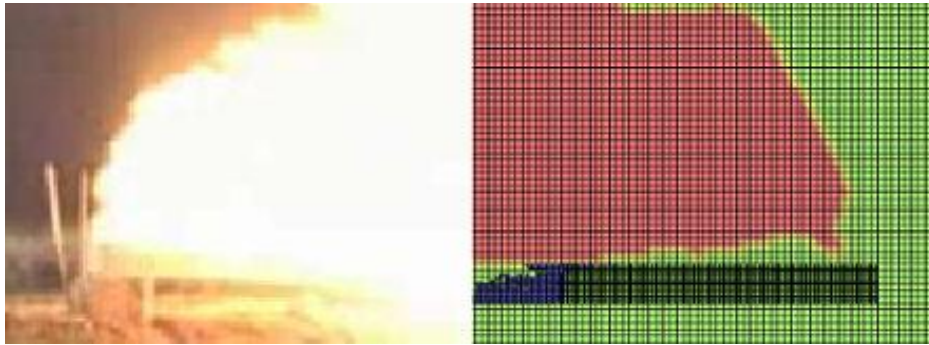


*Fig. 8: Experiment vs. FE model*

### 3.2.2 3D model without reinforcement

As the second step, a 3D plain concrete model was prepared. The model shows great agreement at the surface of the specimen, see. Fig. 9, while the results at the soffit were influenced by missing reinforcement.

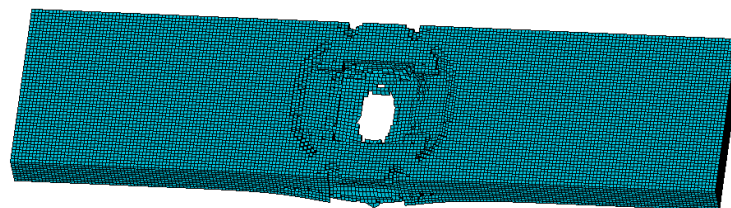


*Fig. 9: Surface of the 2D model without reinforcement*

### 3.2.3 3D model with reinforcement

The 3D reinforced concrete model was prepared to mitigate the weaknesses of the plain concrete model using real dimensions of longitudinal and transverse reinforcement incl. links.

The mesh size was chosen 30mm for concrete and reinforcement and 50mm for air.

The first elements erode when the blast overpressure wave reaches the surface under the hypocenter at 0,25 ms, see Fig. 10.

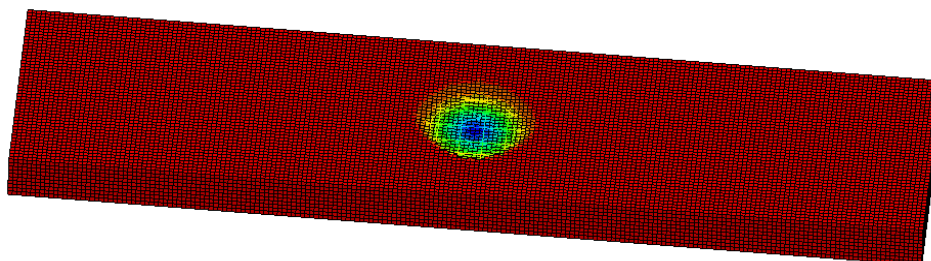


*Fig. 10:* Deflection of the specimen ( $t = 0,25$  ms)

In the following phase, more FE erode, the deflection of the specimen increases and spalling at the soffit takes place. For final results at 1 ms, top surface and soffit, see Fig. 11, 12.

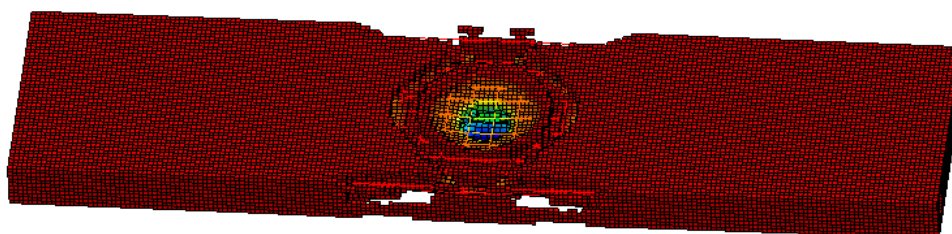


*Fig. 11:* Top view of the specimen after the blast ( $t = 1$  ms)

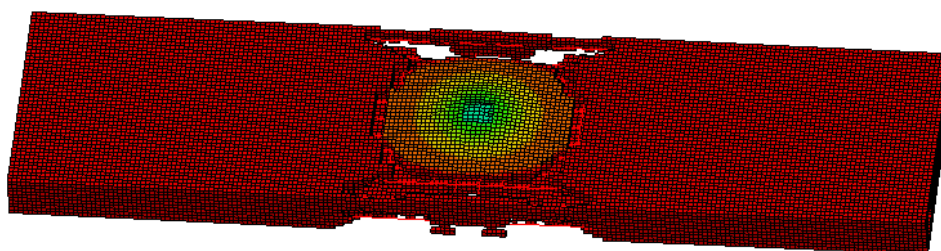


*Fig. 12:* Bottom view of the specimen after the blast ( $t = 1$  ms)

The results show good agreement with the experiments for reinforced concrete specimens. The FE modeling continues for the reinforced fibre concrete specimens.

#### 4. Conclusions

The paper presented results of the field experiments targeted on comparison of blast performance of reinforced concrete and reinforced concrete with plastic fibers. The tests were performed using real scale precast slabs (0,3x1,5x6m) and 25 kg of TNT charges placed in distance from the slab for better simulation of real in-situ conditions.



The results proved beneficiary effect of added fibers on blast performance of the specimens. The puncture on the surface closer to the charge was reduced by 40% in area, the concrete spalling at the soffit of the specimen by 20% in area.

Further, the paper studied methods of FE-modeling the behavior of reinforced concrete specimens and fiber reinforced concrete specimens under blast loading. The conducted numerical study showed the effectiveness of complex 3D models with reinforcement modeled by beam elements.

In the following research, the beneficiary effect of fibre inclusion will be modeled and discussed.

### Acknowledgements

*This paper was supported by the Czech Science Foundation, project No. 103/09/2071, Czech Ministry of Education project MSM 6840770005 and the CTU project No. SGS10/137/OHK1/2T/11.*

### 5. References

- [1] Lawrence Software Technology Corporation, LS-DYNA keyword user's manual, version 971, Livermore Software Technology Corporation, Livermore, CA, USA (2007).
- [2] M. Foglar, E. Sochorová, A. Kohoutková, Field tests of blast performance of reinforced concrete and fibre reinforced concrete specimen, *Engineering mechanics*, May 2011, pp. 143-146
- [3] A.M. Coughlin, E.S. Musselman, A.J. Schokker, D.G. Linzell, Behavior of portable fiber reinforced concrete vehicle barriers subject to blasts from contact charges, *International Journal of Impact Engineering*, Volume 37, Issue 5, May 2010, pp. 521-529
- [4] B. M. Luccioni, R. D. Ambrosini, R. F. Danesi, Analysis of building collapse under blast loads, *Engineering Structures*, Volume 26, Issue 1, January 2004, pp. 63-71
- [5] S.G. Millard, T.C.K. Molyneaux, S.J. Barnett, X. Gao, Dynamic enhancement of blast-resistant ultra high performance fibre-reinforced concrete under flexural and shear loading, *International Journal of Impact Engineering*, Volume 37, Issue 4, April 2010, pp. 405-413
- [6] Y. D. Murray, A. Abu-Odeh, R. Bligh, Evaluation of LS-DYNA Concrete Material Model 159, *Texas Transportation Institute*, May 2007
- [7] J. W.Nam, J.-H. J. Kim, S. B. Kim, N. H. Yi, K. J. Byun, A study on mesh size dependency of finite element blast structural analysis induced by non-uniform pressure distribution from high explosive blast wave, *KSCE Journal of Civil Engineering*, Volume 12, Number 4, 2008, pp. 259-265

**FIBRE CONCRETE 2011**

Prague, 8<sup>th</sup> – 9<sup>th</sup> September 2011

---

